LIVE SOUND LOUDSPEAKER ARRAY OPTIMIZATION FOR CONSISTENT DIRECTIONAL COVERAGE WITH DIFFUSE RADIATION CHARACTERISTICS

AJ Hill — Department of Electronics, Computing & Mathematics, University of Derby, UK
MOJ Hawksford — School of Computer Science and Electronic Engineering, University of Essex, UK

1 INTRODUCTION

Precise control over loudspeaker system directivity is essential in live sound to ensure a consistent listening experience for all audience members[1,2,3] and to limit noise pollution in noise-sensitive areas[4,5]. While loudspeaker array directivity control methods have been well-known for some time[6,7,8,9], industry-standard techniques often result in strong side-lobes and comb-filtering between spaced arrays driven by coherent signals (such as conventional left/right systems), as well as degradation of polar response due to coherent interference from early-reflections in venues[10].

This research aims to adapt a technique developed for polar response control of an array of micro- (or nano-) transducers[11,12] to operate within conventional live sound systems. Section 2 describes the mathematical underpinnings of the signal processing technique (which is an adaptation of one of the author's previous work[11,12]), with Section 3 highlighting key limitations of this approach (as compared to conventional array processing). To avoid unwanted comb-filtering or interference between coherent sources (or early reflections), conversion of the radiation from coherent to diffuse is described and evaluated in Section 4, with the work being concluded in Section 5.

2 POLAR RESPONSE DESIGN

Consider a linear loudspeaker array, as shown in Figure 2.1, consisting of N transducers uniformly spaced by g (m) with the measurement point $P(x,y)$ located a distance from the array. For this analysis, assume each transducer exhibits an omnidirectional polar response over the operational frequency band. The overall array width, w (m), is determined by Equation 2.1.

$$w = (N-1)g \tag{2.1}$$

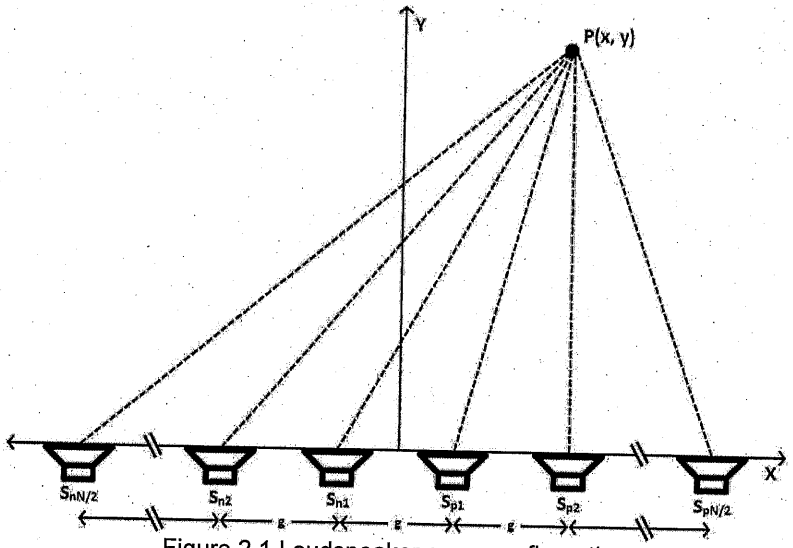

Figure 2.1 Loudspeaker array configuration

Conventional array polar response synthesis requires electronic time delay and/or curvature of the array to ensure the polar response is adequate for the designated coverage area. However, in this paper the array polar response design is handled in a different manner by using an analogy to a finite impulse response filter (FIR).

To develop this analogy, consider the case where idealized array elements are fed a Dirac impulse and the radiated field is observed at a far-field location *P(x,y)* such that the set of incident impulses arriving from the transducers have both equal time offsets and amplitudes. The time offset is a direct function of the location of *P(x,y)* and propagation absorption and boundary reflections have been ignored. An example depicting this simplified configuration is given in Figure 2.2.

By observing the sequence of impulses at the observation point *P(x,y)*, the time-domain response can be likened to the impulse response of a FIR filter where in this example all coefficients are equal. However critical to the development of this analysis and resulting directly from the geometry is that the effective filter sampling period is a function of polar angle. Now assume the FIR filter has a low-pass filter response where the shape is defined by the coefficients but with the frequency scale dependent on the sampling period, consequently if the sampling rate decreases then the filter cut-off frequency falls in direct proportion. The key observation therefore is that as the observation point *P(x,y)* sweeps over the measurement circle, the effective sampling period and cut-off frequency change.

So for the present example, as the sample period increases as *P(x,y)* moves off axis, the effective FIR filter cut-off frequency falls. The cut-off frequency defines the transition from passband to stopband or attenuation region within the polar response. In addition, if the feeds to each drive unit also include a transfer function, then it is possible to achieve a high degree of control over the array polar response.

To fully develop this analytical process there is a further caveat that must be considered. If the coefficients forming the FIR filter were equal at all frequencies, then since the cut-off frequency is a function of location *P(x,y)* it would follow that the polar response is strongly frequency dependent. In an array it is desirable that the polar response is not strongly dependent on frequency. Consequently the array coefficients must themselves be made frequency dependent. In other words the frequency responses for each location of *P(x,y)* should be as closely matched as possible.

Assuming the equi-coefficient array is observed in the extreme far field (a more precise definition of this will be explored in Section 3.3), the effective FIR filter sampling rate (F_s) for a Dirac input can be predicted at an arbitrary angle, θ, off-axis from normal to the array (Equation 2.2).

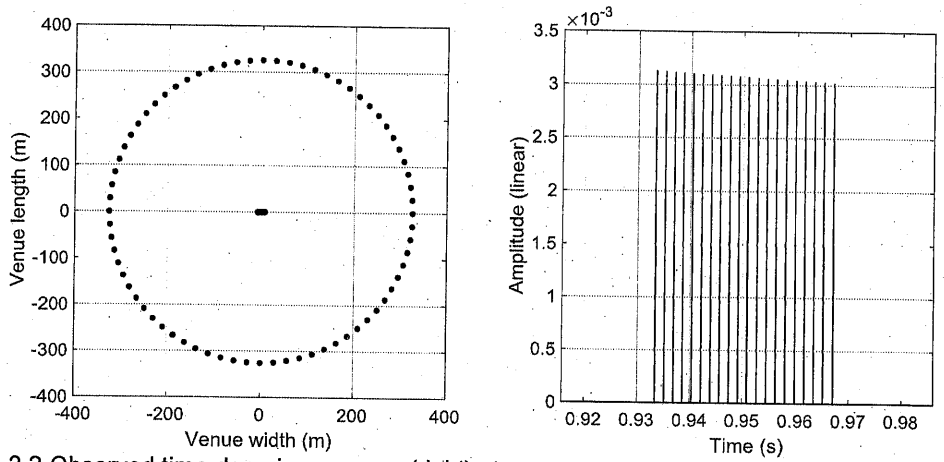

Figure 2.2 Observed time domain response (right) at measurement point (indicated by red dot in left figure) located at 20 times the array width. 20-unit array inspected (indicated in blue on left figure)

$$Fs(\theta) = \frac{g \sin\theta}{c} \tag{2.2}$$

where c represents the speed of sound in air (m/s). For an unprocessed array, the cut-off frequency of the spatially-based FIR filter is position-dependent and can be calculated using Equation 2.3. An analysis of cut-off frequency versus angle off-axis from normal to the array is given in Figure. 2.3.

$$f_c(\theta) = \frac{c}{2g \sin\theta} \tag{2.3}$$

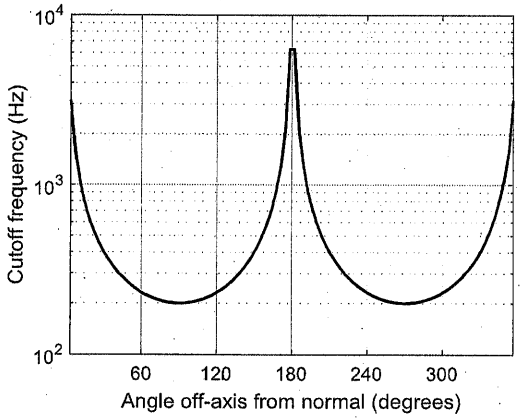

Figure 2.3 Array cut-off frequency vs. observation angle off-axis from normal

The example array contains 20 transducers spaced at 0.8575 m (half-wavelength of 200 Hz). At 90° off-axis from normal, it can be seen that the predicted cut-off frequency of the array is 200 Hz. The maximum spacing of transducers within the array (g_{max}) is based on the upper limit of the array's frequency range and is calculated with Equation 2.4. As long as spacing, g, is equal to or less than g_{max}, the array will be effective up to the desired frequency limit.

$$g_{\max} = \frac{c}{f_c(90°)} \tag{2.4}$$

The lower frequency limit of the array is approximately defined by the array width, whereby the frequency with a full wavelength equal to the array width is roughly the lower limit for precise array polar response control. This will be investigated in Section 3.2.

The key to designing the array's polar response is by treating the array elements as taps in an FIR filter is to take note that for ideal operation the polar response's passband should terminate at the same angle off-axis at all frequencies within the operational band. To achieve this, frequency dependent complex coefficients must be determined so that the observed cut-off frequency matches the frequency under inspection at the spatial passband edge.

A direct calculation of the complex coefficients can be performed by noticing that if a sampled sinc function were to be observed at the measurement point, this would represent a "brick-wall" low-pass filter. In reality only a windowed sampled sinc function is possible since there are a finite number of array elements. Consequently, if the number of elements in the array is decreased, the polar-response transition region broadens as the filter characteristic is degraded.

As an example, the coefficients of each of the transducers in the example 20-unit array were set so that they reflect a windowed sinc pulse and analysed along the perimeter of a circle with radius 20 times the array width (Figure. 2.4).

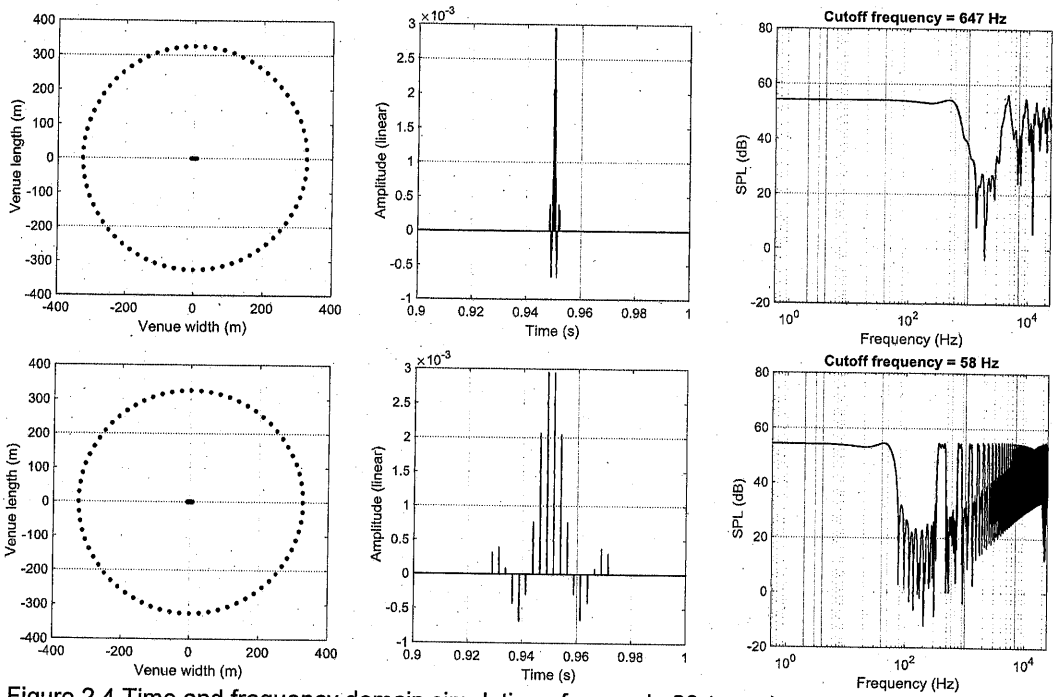

Figure 2.4 Time and frequency domain simulation of example 20-transducer array at 5° (top) and 90° (bottom) off-axis from normal

The application of frequency-independent sinc function-defined coefficients gives an angular-dependent cut-off frequency for the array. Note that above the cut-off frequency there is a stopband followed by spatial aliasing distortion. This will manifest itself as unwanted high frequency side lobes in the polar response.

The frequency-dependent transducer coefficients are calculated as follows, one frequency at a time. First, observe that the finite Fourier transform (FFT) of the N-point observed response has a frequency resolution as defined by Equation 2.5.

$$f_{res} = \frac{2f_c}{N} \tag{2.5}$$

The desired polar response requires coefficient definition based on the edge of the spatial passband. If the desired beamwidth is L, then the passband spatial edge is located at $L/2$ (assuming the beam is directed straight forward). The spatial sampling rate, f_s, at this position can be determine with Equation 2.6.

$$f_s = \frac{c}{g\sin(L/2)} \tag{2.6}$$

Solving Equation 2.4 for c and substituting into Equation 2.6, results in the equation for sample rate (Eq. 2.7).

$$f_s = \frac{g_{\max} f_c}{g\sin(L/2)} \tag{2.7}$$

Assuming the target is as close to a brick wall response as possible, the frequency response's passband must terminate at the nearest frequency bin to the current analysis frequency, f Hz. This frequency bin is notated as n_c and is calculated using Equation 2.8. If necessary, linear interpolation can be applied to either side of n_c, to limit error due to the frequency resolution being restricted to the number of transducers in the array.

$$n_c = \left\lceil \frac{f}{f_s} N \right\rceil = \left\lceil \frac{fg}{f_c g_{\max}} N \sin\left(\frac{L}{2}\right) \right\rceil \tag{2.8}$$

The generation of the required sync function can be applied in the frequency domain as a spectral mask, following Equation 2.9. Note that Equation 2.9 assumes Matlab indexing whereby the first element in an array is indexed as n = 1.

$$w_f(n) = \begin{cases} 1, & \text{if } \mathrm{n} \le \mathrm{n}_c \\ 0, & \text{if } \mathrm{n}_c < n \le N - (n_c - 1) \\ 1, & \text{otherwise} \end{cases} \tag{2.9}$$

Assuming that coherent radiation is desired, the FFT of a Dirac impulse, X_{in}, is normalized and windowed with w_f before being translated back to the time domain with an IFFT and windowed to avoid non-zero coefficients at the edges of the array (which would result in spectral leakage), following Equation 2.10. In this implementation, the array coefficient window, w_a, is a raised cosine. This calculation results in the necessary array coefficients for current analysis frequency, f Hz.

$$a_f = w_a \mathcal{F}^{-1}\left(w_f\left(\frac{X_{in}}{\max(|X_{in}|)} \right) \right) \tag{2.10}$$

Lastly, to ensure unity gain on-axis across all frequencies in the operational band, the calculated coefficients in a_f are equalized (Equation 2.11). Note that it is possible to steer the generated beam and or to create multiple beams from a single array. This isn't explored in this paper, but a full description of the implementation of such features is described in one of the author's previous works[11,12].

$$a_{f,norm} = \frac{a_f}{\sum_{n=1}^{N} a_f} \tag{2.11}$$

In the case of this specific application where the main radiation lobe is directed on-axis, the calculated coefficients will be purely real.

As an example, consider the 20-transducer array spaced so that the upper limit of the operation band is 200 Hz. This results in an array that is 16.3 m wide, corresponding to the full-wavelength of 21 Hz. The transducer coefficients for a beamwidth of 60° are shown in Figure 2.5. Note that the coefficients are symmetrical about the center of the array, therefore only coefficients for the first half of the array are plotted. The predicted polar response (still analysed at 20 times the width of the array) is given in Figure 2.6.

The coefficients all fall within the range of ±1, although it must be noted that after application of these coefficients, the mean amplitude generated by each transducer will be less than those for the unprocessed array, where all coefficients equal 1. This reduces efficiency of the loudspeaker array and will be explored in more detail in Section 3.4.

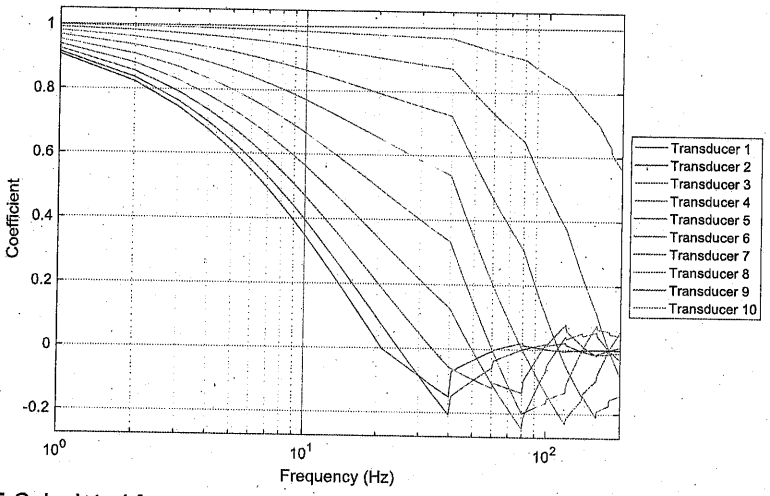

Figure 2.5 Calculated frequency-dependent transducer coefficients (unequalized) for a 20-transducer array spaced for operation up to 200 Hz and a beamwidth of 60° (only first half of the array's coefficients shown due to symmetry)

Inspection of the simulated polar response over frequency indicates that a 60° beam has been achieved from approximately 30 – 200 Hz. There is, on average, 40 dB attenuation in the spatial stopband. Ripples shown in the stopband are due to the method of windowing applied to the array coefficients. In this case, windowing is applied to the outside three transducers on either side of the array. Increasing the window length will decrease the stopband ripples (windowing is possible up to the full array width). This will be explored further in Section 3.4.

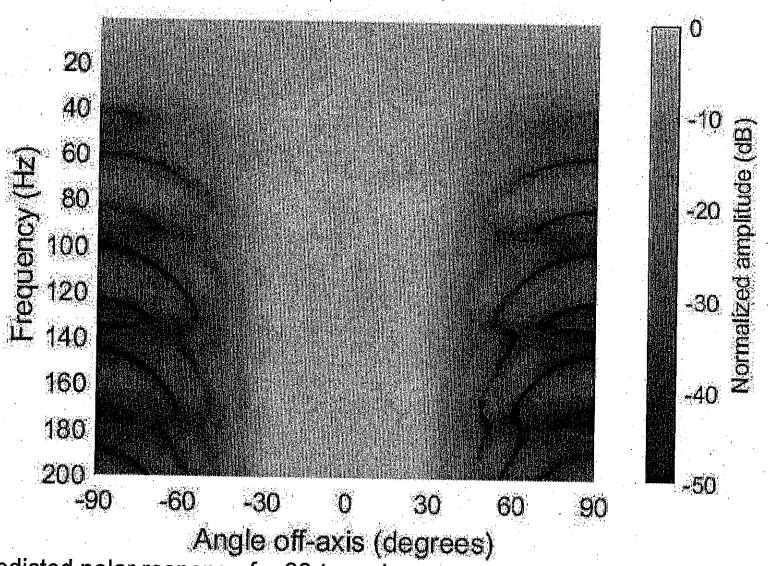

Figure 2.6 Predicted polar response for 20-transducer array spaced for operation up to 200 Hz and a beamwidth of 60°

3 METHOLDOLOGY LIMITATIONS

Limitations exist in the implementation of array beamforming, where compromises must usually be made to allow for a practical implementation. This section describes four important limitations for this technique: transducer spacing, array width, measurement distance and system efficiency.

3.1 Transducer spacing

The maximum frequency that can be controlled by the array is defined by the interspacing of the transducers. Since the greatest observed spacing (from the vantage point of the measurement circle) occurs at ±90° off-axis, the maximum frequency can be calculated using Equation 3.1.

$$f_{\max} = \frac{c}{2g} \tag{3.1}$$

Since the frequency domain derivation of the array coefficients is based on the number of taps (transducers) available and the upper frequency limit, as dictated by the inter-transducer spacing, no coefficients are calculated above this limit since this would be above Nyquist for the spatially configured filter (loudspeaker array). Figure 3.1 shows the relationship between required inter-element spacing and upper frequency limit for array steering.

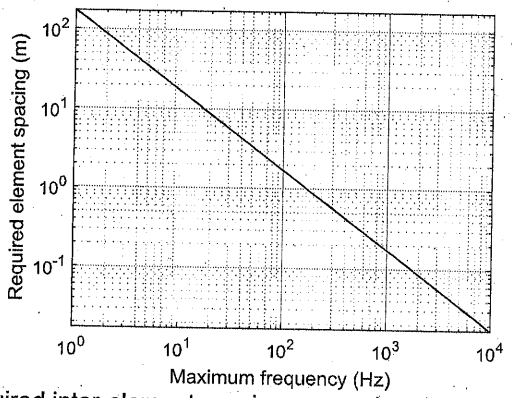

Figure 3.1 Required inter-element spacing vs. maximum controllable frequency

At very low frequencies, the required spacing surpasses 10 m (and in some cases 100 m), which isn't necessarily practical. Towards the upper end of the spectrum, elements need to be spaced within a few mm of each other which is also unlikely to be practical, both in terms of the finite size of a transducer as well as the number of transducers required to allow for wide bandwidth operation (a limitation that isn't as serious for RF antennas, where similar array optimization is used). It can therefore be judged that a reasonable upper frequency range for such an array, as applied to a conventional live sound system, could be 40 Hz – 2 kHz (corresponding to transducer spacing from 4.3 m down to 8.6 cm, respectively).

3.2 Array width

If a high upper frequency is required, inter-element spacing will be very small, thus requiring many transducers to permit the array to operate over a wide bandwidth. If the desired upper frequency range and maximum allowable array width is defined by a system designer, then the required number of elements and the minimum operation frequency can be calculated using Equations 3.2 and 3.3, respectively. Figure 3.2 (left) highlights the relationship between minimum/maximum controllable frequency and the number of transducers required within the array, while Figure 3.2 (right) relates minimum controllable frequency to required array width.

$$N = \left\lfloor \frac{w_{\max}}{g} \right\rfloor + 1 \tag{3.2}$$

$$f_{\min} = \frac{c}{g(N-1)} \tag{3.3}$$

This analysis is critical in determining the practicality of a system. Clearly, it isn't practical (in live sound, at least) to attempt to control 10 Hz – 1 kHz, since this would require 200 transducers over a width of 34.3 m. This width may be possible for arena-based events, but it's unlikely that a 200-transducer array would be feasible. In live sound, arrays don't typically extend beyond 40 elements.

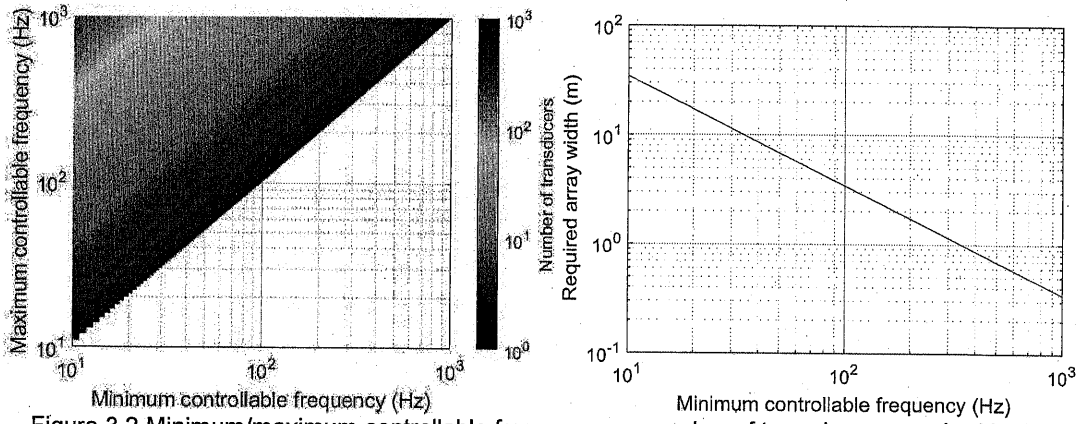

Figure 3.2 Minimum/maximum controllable frequency vs. number of transducers required in the loudspeaker array for proper operation (left) and required loudspeaker array width vs. minimum controllable frequency (right)

3.3 Measurement distance

Thus far the array's performance has been observed in the extreme far field (20 times the array width, in this case). Audience members don't typically listen to an event over 300 m away from a stage. The audience is usually located within 100 m of a stage. If an audience extends beyond this, delay loudspeakers are utilized.

The example 20-transducer array was analysed from 1 m (6% of the array width) to 1000 m (6000% of the array width) in terms of mean stopband attenuation and beamwidth error (Figure 3.3). The data indicates that for this particular configuration the array performs as expected at distances greater than 3 m (approximately 20% of the array width) and at frequencies above 40 Hz. The issue of sidelobes (as evident in Figure 2.6) are a consequence of the sinc pulse truncation (due to the finite length of the array), as disused earlier.

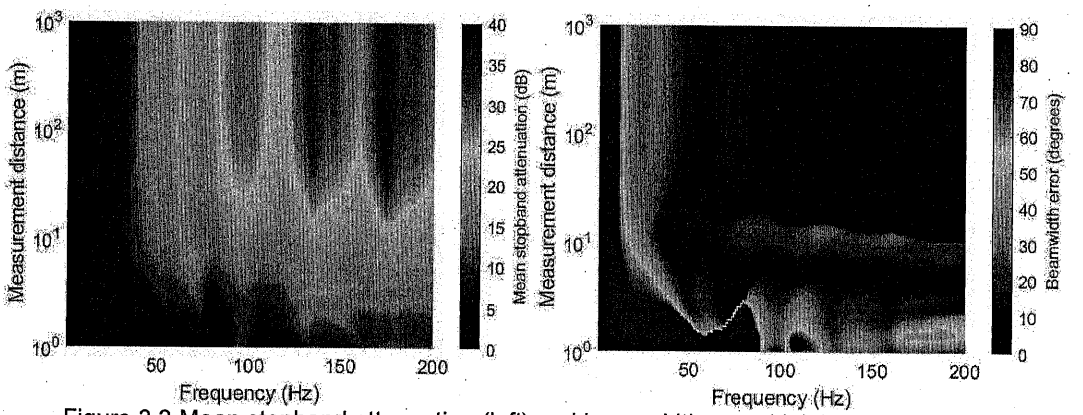

Figure 3.3 Mean stopband attenuation (left) and beamwidth error (right) as a function of measurement distance and angle off axis from normal to the 20-transducer array

3.4 System efficiency

System efficiency can be difficult to define in the context of live sound. In one sense, a system can be inspected electronically, whereby any limitation to the signal sent from a power amplifier to a loudspeaker can be considered a loss of efficiency. Such is the case with the coefficients shown in Figure 2.5. The unprocessed system has coefficients set to unity, sending a full signal to all transducers. Any reduction from this could be considered a loss of efficiency.

The issue with this form on analysis is that it neglects the primary goal in live sound which is to deliver a position-independent listening experience to the entire audience area. Although it isn't ideal to limit signals feeding certain transducers in the array, if this helps to achieve even coverage across the audience, it can be argued to be a good thing (provided the overall desired output level can still be achieved while maintaining sufficient system headroom).

To inspect system efficiency (in terms of consistency of audience coverage and overall output level), mean output level was calculated for both the unprocessed and processed array, where the audience was defined as being located within the target 60° beamwidth and from 3 – 100 m from the array (Figures 3.4 & 3.5). To allow a direct comparison, the signal normalization step was bypassed and propagation attenuation was ignored.

The unprocessed system results in a mean output level across the entire audience area and operational frequency band (40 – 200 Hz) of 107.5 dB with a mean spatial variance of 11.1 dB across the audience. The processed system results in a mean output level across the entire audience area and operation frequency band of 93.4 dB with a mean spatial variance of 0.4 dB across the audience.

To match the output of the unprocessed array, an overall voltage gain of 14.1 dB is required. If this were feasible (which could be difficult for some systems), then the mean output level across the audience and operational frequency range will be 107.5 dB with spatial variance of 0.5 dB across the audience area (Figure 3.5).

The unprocessed system is likely to meet the target output level requirements for a live sound system (this scenario assumes the peak output of each transducer is 93.4 dB), but fails in terms of sound distribution consistency across the audience. The processed system, on the other hand, achieves good consistency across the audience, but only generates the peak output of any one transducer (or requires gain to match the unprocessed system's output).

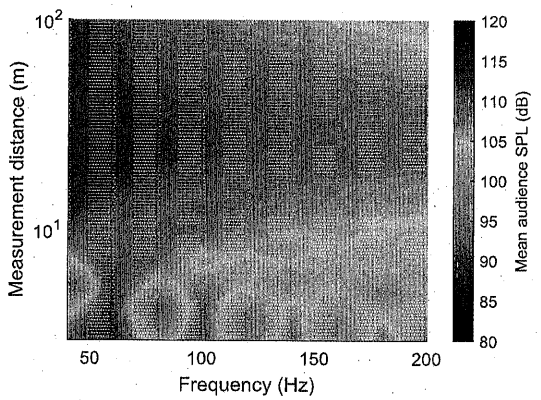

Figure 3.4 Mean audience SPL as a function of measurement distance and frequency for the unprocessed 20-transducer array

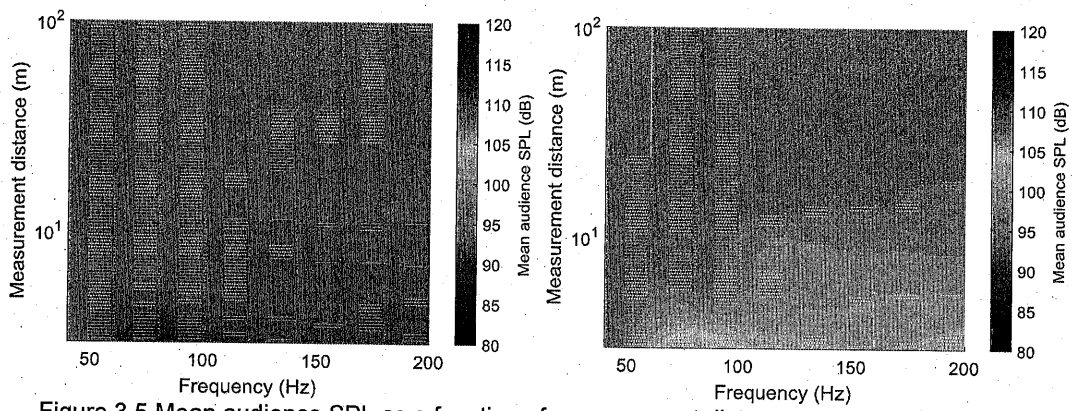

Figure 3.5 Mean audience SPL as a function of measurement distance and frequency for the processed 20-transducer array with no additional gain (left) and with 14.1 dB make-up gain (right)

4 DIFFUSE RADIATION

Assuming that the decreased system efficiency due to the Fourier-based beamforming is manageable (i.e. there's ample system headroom to allow for make-up gain), additional issues can be inspected. A common problem in live sound reinforcement is coherent interference between spaced sources or arrays. Consider a left/right configuration of subwoofers or line arrays. In most cases, the bulk of the source material is mixed as multiple mono due to difficulties in delivering accurate stereo content to a wide audience area (although this may be changing with the introduction of hyper-realistic source-based sound reinforcement systems such as L-Acoustics L-ISA[13] and d&b audiotechnik Soundscape[14]).

The problem in this sort of situation is that the signals emitted from the left and rights sides of the sound system are highly-correlated. This results in a position dependent magnitude response and prevents consistent coverage across an audience. A solution to this problem is to decorrelate the left and right signals in such a way as to avoid the bulk of the negative coherent interference effects without perceptually coloring the audio signal. Additionally, it must be noted that such decorrelation, when applied, will eliminate most coupling between adjacent transducers, which will further limit system efficiency.

An additional problem encountered when applying beamforming to a loudspeaker array is the negative influence of early-reflections in a closed space. Strong lateral early reflections will often corrupt the loudspeaker directivity that would have otherwise been as desired in a free-field. Addressing this issue is less straightforward as the coherent interference problem. In this case, even if decorrelation were applied to the array, the early-reflections would be correlated with the direct sound. This is unlikely to help the situation. Instead, there needs to be a way of decorrelating the direction sound with the early-reflections. In essence, instead of spatially-based decorrelation (which was required for the coherency issue), time-based decorrelation is required[10].

A possible solution to both the above issues will be discussed in this section, with two different implementations, highlighting the level of practicality and effectiveness of each.

4.1 Implementation

There are a number of decorrelation methods available for use in this instance. Recent developments in a decorrelation method originally developed for diffuse-mode loudspeakers (DMLs), termed diffuse signal processing (DiSP)[15], have proven this method to be effective in limiting signal correlation (both spatially and temporally) while minimizing perceptual coloration to the audio signal[10].

DiSP operates by generating a library of what are known as temporally diffuse impulses (TDIs). The generation of these TDIs won't be detailed here, but details can be found in recent work by one of the authors[10]. Once the TDI library has been generated, DiSP can be applied to a system in either a static or dynamic manner.

For static applications, one TDI is applied to each transducer in the sound system. The application can either be via direct convolution or as a FIR approximation of the TDI. Once applied to the source signal, the system elements will be decorrelated from each other, decreasing the negative effects of coherent interference, at the expense of some system efficiency. Interference from early-reflections will still be problematic.

For dynamic applications, one TDI is applied to each transducer in the sound system for each time window within a real-time processor. From there, a new TDI from the library is randomly applied to each transducer at an update rate in line with the arrival of the first problematic early reflections, with a number of interpolation steps between TDIs to ensure a smooth transition. This process has been shown to decorrelate the direct signals from system elements as well as the direct sound and early reflections within a venue[10]. This has a good chance of solving both of the problems listed above. If done correctly, there will be negligible audio signal coloration and minimal negative impact to system efficiency.

4.1.1 Direct

Direct implementation of decorrelation within the beamforming algorithm was introduced in the original work describing this method[11]. Instead of applying the spectral brick-wall mask to the FFT of a Dirac impulse, the spectral mask is applied to the FFT of a TDI. Since the algorithm operates one frequency at a time, there is no need to generate a complete TDI (or library of TDIs). Instead, randomized phase noise is applied to the Dirac impulse (which is centred in the time window), where the phase noise can exhibit values between $\pm\pi$ radians (this could be adjusted to any value, but this range has been investigated in this and prior work and has been found to be effective). Originally, the beamforming algorithm frequency resolution was limited by the number of transducers. With such a limitation, the coefficients and polar response at a radius of 25 m are given in Figure 4.1.

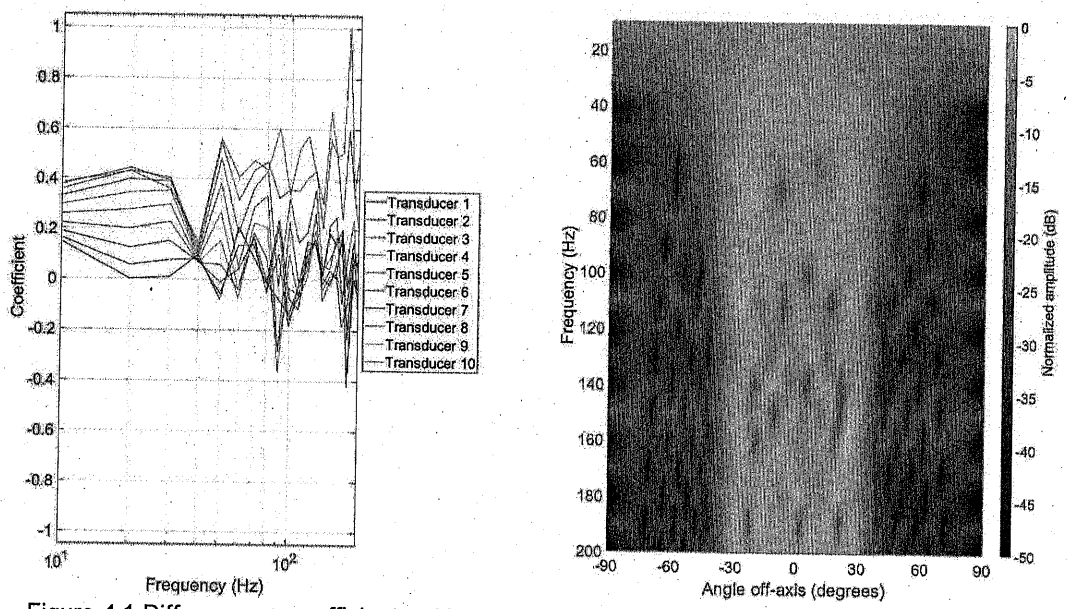

Figure 4.1 Diffuse array coefficients with 20 frequency analysis bins (right) and corresponding predicted far-field polar response (left)

While the upper frequency range shows coefficients exhibiting strong randomization, the lower portion of the spectrum does not. This is indicated within the polar response with little to no decorrelation observed below approximately 60 Hz. Above this frequency, diffuse behaviour can be observed, but there are potentially perceptible peaks and dips in the response due to the course nature of the frequency analysis within the beamforming algorithm. To eliminate these issues, the number of analysis frequency bins can be increased to 400, improving the frequency resolution from 10 Hz to 0.5 Hz. The results are shown in Figure 4.1.

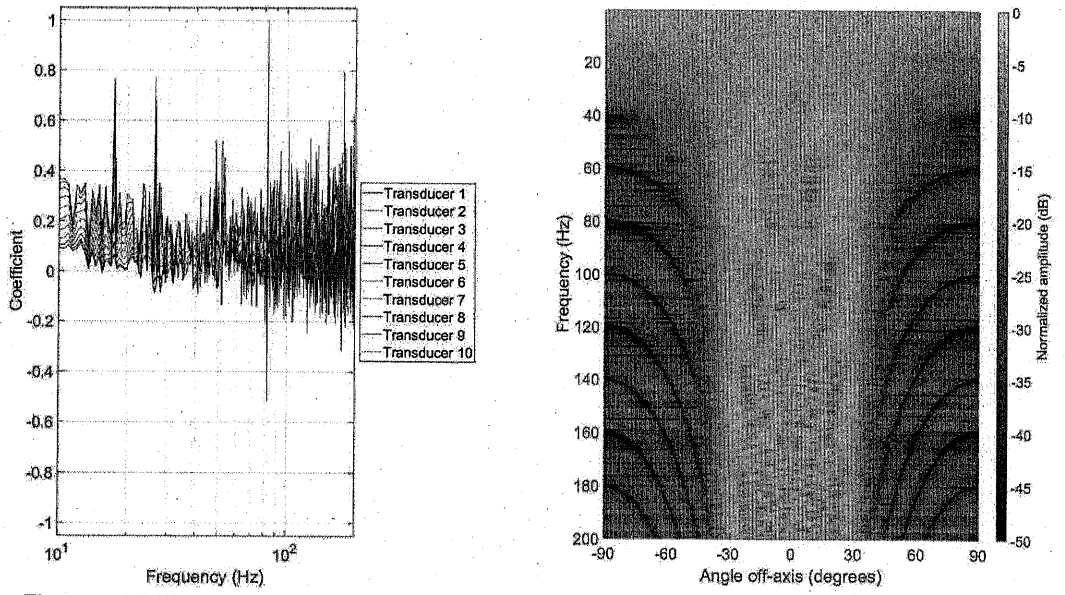

Figure 4.1 Diffuse array coefficients with 400 frequency analysis bins (right) and corresponding predicted far-field polar response (left)

Now the predicted polar response is much closer to that of the coherent signal configuration in Figure 2.6. The sidelobes are present as before, which again can be attenuated by windowing the coefficients towards the ends of the array. The peaks/dips due to the diffuseness of the signal are smaller in size and aren't likely to be perceptible (past research has found that 1/9 octave smoothing is appropriate in the low-frequency range[16]). Diffuse nature is now observed down to approximately 40 Hz, which is roughly the limit of this array's operation band.

The diffuse array's mean audience level in this case is 92.0 dB with a mean spatial variance of 5.0 dB across the audience (Figure 4.2, left). Perceptually, the variance is likely to be much less, as the observed peaks/dips are narrow, both spatially and spectrally. The mean output level is as expected: 1.4 dB lower that the coherent array due to the reduction of inter-element coupling due to the decorrelation applied. As before, this would require a significant amount of make-up gain to compensate for the reduced efficiency of the algorithm.

As a potential workaround to the reduction in efficiency, the on-axis equalization (Equation 2.11) can be bypassed. This will result in the array's resulting magnitude response favoring the lower frequency range, but allows for the coefficients to remain closer to unity. The predicted mean output level across an audience for this approach is given in Figure 4.2 right (102.4 dB mean output level; 11.7 dB mean spatial variance across the audience).

While this direct implementation of decorrelation to the array can ensure that spaced arrays or clusters of transducers won't exhibit severe coherent interference, it does nothing in the way of reducing the impact early-reflections can have on the polar response, due to the static nature of the decorrelation applied within the array coefficients. A different approach is therefore required.

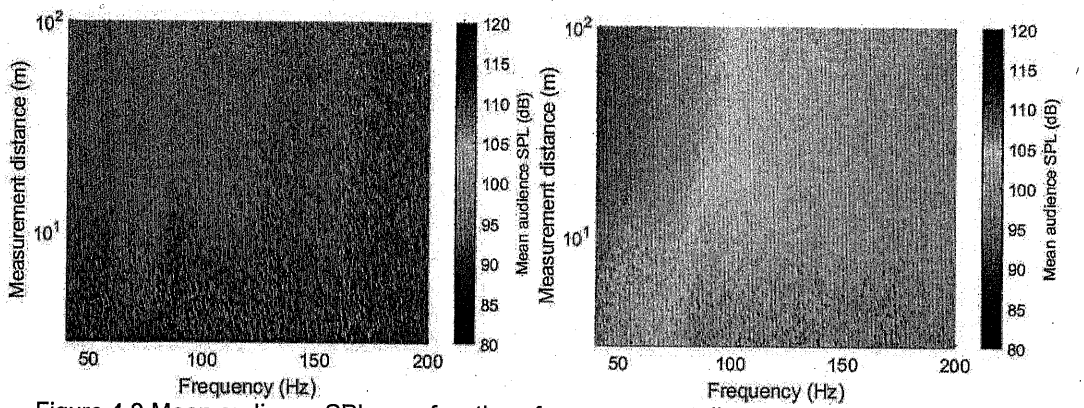

Figure 4.2 Mean audience SPL as a function of measurement distance and frequency for the processed diffuse 20-transducer array with (left) and without (right) on-axis equalization

4.1.2 Indirect

In order to overcome the inability of the direct application of decorrelation to the array beamforming algorithm to handle time-varying decorrelation, an indirect application of decorrelation is necessary. The implementation of this is straightforward. The beamforming algorithm is executed, which when complete, provides impulse responses that must be real-time convolved with each transducer's input signal. Two example impulses are shown in Figure 4.4, again for the 20-transducer array.

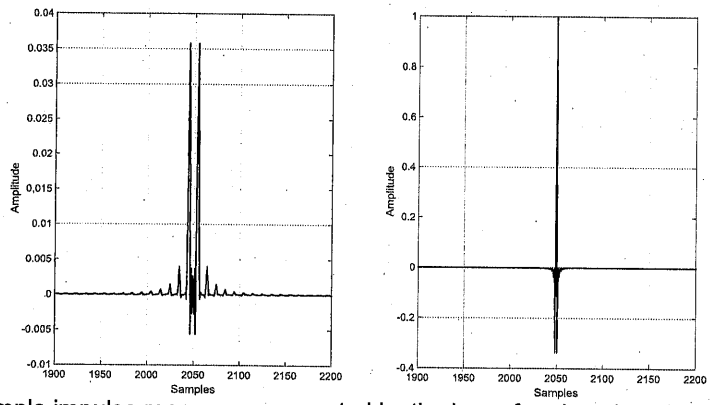

Figure 4.4 Example impulse responses generated by the beamforming algorithm for the first (left) and tenth (right) element in the 20-transducer array

With these impulse responses in hand, all that is necessary to apply dynamic DiSP[10] is to convolve these impulses by the appropriate TDIs drawn from the TDI library. This process can take place in real-time, with decorrelation varying time frame to time frame. Such an approach would solve both the coherent interference and early-reflection issues.

5 CONCLUSIONS

A loudspeaker array beamforming approach originally developed for use within 2D digital loudspeaker arrays consisting of micro- or nano-transducers has been adapted to operate within conventional live sound systems. The algorithm has been described with a preliminary analysis of carried out, indicating that while the array's coverage pattern can be tightly controlled over a wide frequency range, the core issue is the reduction in system efficiency.

This topic has the potential, however, to solve a central problem in array beamforming, that being corruption of directionality due to early-reflections within performance venues. The inclusion of

decorrelation in an indirect manner allows for the direct sound from the array to be decorrelated from any problematic early-reflections, this on top of preventing the common issue of coherent interference between spaced arrays or clusters of sources (causing a position-dependent listening experience in the audience).

Further work is required in the following areas as follows:

- Precise definition of lower frequency for accurate array control (if possible)
- Simulated application of array beamforming and static DiSP, to inspect if problems due to coherent interference of spaced arrays or clusters of transducers have been neutralized
- Simulated application of array beamforming and dynamic DiSP, to inspect if problems due to early reflections have been neutralized
- Optimization of algorithm to minimize sidelobes while maintaining reasonable efficiency
- Construction of a scale version of an array for practical experiments.

6 REFERENCES

1. Hill, A.J.; M.O.J. Hawksford, A.P. Rosenthal; G. Gand. "Subwoofer positioning, orientation and calibration for large-scale sound reinforcement". 128th AES Convention, London, UK. May, 2010.
2. Hill, A.J. "Practical considerations for subwoofer arrays and clusters in live sound reinforcement". 3rd International Conference on Sound Reinforcement – Open Air Venues, Struer, Denmark. August, 2017.
3. Hill, A.J. "Live sound subwoofer system performance quantification". 144th Convention of the Audio Engineering Society, Milan, Italy. May, 2018.
4. Christner, M.; J. Schaal; D. Zollitsch; E. Shabalina; D. Belcher. "Far-field noise prediction for open-air events. Part 1: Background and propagation models." 142nd Convention of the Audio Engineering Society, Berlin, Germany. May 2017.
5. Belcher, D.; M. Christner; E. Shabalina. "Noise Prediction Software for Open-Air Events Part 2: Experiences & Validation." 142nd Convention of the Audio Engineering Society, Berlin, Germany. May 2017.
6. Eargle, John. "Loudspeaker Handbook – Second Edition." Kluwer Academic Publishers. New York, USA. 2003.
7. Ureda, M.S. "Analysis of loudspeaker line arrays." Journal of the Audio Engineering Society, vol. 52, no. 5, pp. 467-495. May 2004.
8. Aarts, R.M.; A.J.E.M. Janssen. "On analytic design of loudspeaker arrays with uniform radiation chracteristics." Journal of the Acoustical Society of America, vol. 107, no. 1, pp. 287-292. January 2000.
9. Van Der Wal, M.; E.W. Start; De Vries, D. "Design of logarithmically spaced constant-dirctivity transducer arrays." Journal of the Audio Engineering Society, vol. 44, no. 6, pp. 497-507. June 1996.
10. Moore, J.B.; A.J. Hill. "Dynamic diffuse signal processing for low-frequency spatial variance minimization across wide audience areas." 143rd Convention of the Audio Engineering Society, New York, USA. October, 2017.
11. Hawksford, M.O.J. "Smart Digital Loudspeaker Arrays." Journal of the Audio Engineering Society, vol. 51, no. 12, pp. 1133-1162. December 2003.
12. Hawksford, M.O.J. "Smart directional and diffuse digital loudspeaker arrays." 110th Convention of the Audio Engineering Society, paper 5362. May 2001.
13. L-Acoustics L-ISA. http://www.l-isa-immersive.com/
14. d&b audiotechnik Soundscape. https://www.dbsoundscape.com/
15. M.O.J. Hawksford, N. Harris, "Diffuse signal processing and acoustic source characterization for applications in synthetic loudspeaker arrays." 112th Convention of the Audio Engineering Society, paper 5612. May 2012.
16. Moore, J.B.; A.J. Hill. "Optimization of temporally diffuse impulses for decorrelation of multiple discrete loudspeakers". 142nd Convention of the Audio Engineering Society, Berlin, Germany. May, 2017.